ΔF508 CFTR Pool in the Endoplasmic Reticulum Is Increased by Calnexin Overexpression

Tsukasa Okiyoneda,* Kazutsune Harada,* Motohiro Takeya,[†] Kaori Yamahira,* Ikuo Wada,[‡] Tsuyoshi Shuto,* Mary Ann Suico,* Yasuaki Hashimoto,* and Hirofumi Kai*[§]

Departments of *Molecular Medicine and [†]Pathology, Graduate School of Medical and Pharmaceutical Sciences, Kumamoto University, Kumamoto 862-0973, Japan; and [‡]Department of Cell Science, Institute of Biomedical Sciences, Fukushima Medical University School of Medicine, Fukushima 960-1295, Japan

The most common cystic fibrosis transmembrane conductance regulator (CFTR) mutant in cystic fibrosis patients, ΔF508 CFTR, is retained in the endoplasmic reticulum (ER) and is consequently degraded by the ubiquitin-proteasome pathway known as ER-associated degradation (ERAD). Because the prolonged interaction of ΔF508 CFTR with calnexin, an ER chaperone, results in the ERAD of ΔF508 CFTR, calnexin seems to lead it to the ERAD pathway. However, the role of calnexin in the ERAD is controversial. In this study, we found that calnexin overexpression partially attenuated the ERAD of ΔF508 CFTR. We observed the formation of concentric membranous bodies in the ER upon calnexin overexpression and that the ΔF508 CFTR but not the wild-type CFTR was retained in the concentric membranous bodies. Furthermore, we observed that calnexin overexpression moderately inhibited the formation of aggresomes accumulating the ubiquitinated ΔF508 CFTR. These findings suggest that the overexpression of calnexin may be able to create a pool of ΔF508 CFTR in the ER.

INTRODUCTION

Cystic fibrosis transmembrane conductance regulator (CFTR) is a polytopic integral membrane protein that functions as a cAMP-dependent Cl⁻ channel in the apical membrane of epithelial cells (Anderson *et al.*, 1991; Drumm *et al.*, 1991; Tabcharani *et al.*, 1991; Bear *et al.*, 1992). Mutations in the CFTR gene lead to the absence or malfunction of a regulated Cl⁻ channel in the apical membrane of secretory epithelia, resulting in the clinical symptoms of cystic fibrosis (CF) (Kerem *et al.*, 1989; Riordan *et al.*, 1989; Rommens *et al.*, 1989; Cheng *et al.*, 1990). Therefore, potential CF therapies are aimed at overcoming the functional impairment of various mutant CFTRs, particularly ΔF508 CFTR, in which a phenylalanine at position 508 is deleted from the first nucleotide-binding fold. This mutation is found in ~70% of CF chromosomes and results in a severe form of the disease; >90% of CF patients have at least one ΔF508 allele (Tsui, 1992; Sferra and Collins, 1993). Although ΔF508 CFTR is functionally competent as a cAMP-dependent Cl⁻ channel in model situations where it reaches the plasma membrane (Drumm *et al.*, 1991; Denning *et al.*, 1992; Li *et al.*, 1993), in mammalian cells ΔF508 CFTR fails to reach the plasma membrane.

CFTR biogenesis is inefficient. During insertion into the ER membrane, CFTR interacts with the cytosolic chaperones Hsc70/Hdj-2 and Hsp90, as well as the ER chaperone calnexin (CNX) (Yang *et al.*, 1993; Pind *et al.*, 1994; Loo *et al.*, 1998; Meacham *et al.*, 1999). After ATP-dependent conformational maturation, assisted by cytosolic and ER chaperones, the chaperones release CFTR, and only ~30% of the immature wild-type (wt) CFTR transits to the late secretory pathway, ultimately reaching the plasma membrane (Lukacs *et al.*, 1994). However, most of the immature wt CFTR (~70%), and nearly all of immature ΔF508 CFTR, fail to mature and do not transit to the late secretory pathway (Lukacs *et al.*, 1994). They are trapped in the ER as core-glycosylated products (~140 kDa) and are ultimately degraded by the ER-associated degradation (ERAD) pathway. In fact, CFTR retained in the ER is ubiquitinated and retrotranslocated to the cytosol where it undergoes proteasomal degradation (Jensen *et al.*, 1995; Knittler *et al.*, 1995; Johnston *et al.*, 1998; Gelman *et al.*, 2002).

The lectin-like chaperone calnexin participates in the ER retention and ERAD of ΔF508 CFTR (Pind *et al.*, 1994). Calnexin is a type I transmembrane protein localized in the ER that associates selectively with incompletely folded glycoproteins containing monoglucosylated N-linked oligosaccharides (Wada *et al.*, 1991). Calnexin transiently interacts with newly synthesized CFTR and dissociates after it attains a native conformation (Pind *et al.*, 1994). If CFTR cannot attain a native conformation, as is the case for ΔF508 CFTR, calnexin fails to dissociate from the misfolded CFTR (Pind *et al.*, 1994). The prolonged interaction of ΔF508 CFTR with calnexin results in

Abbreviations used: CF, cystic fibrosis; CFTR, cystic fibrosis transmembrane conductance regulator; ER, endoplasmic reticulum; ERAD, endoplasmic reticulum-associated degradation; IB, inclusion body; CM body, concentric membranous body.

the ERAD of ΔF508 CFTR (Pind *et al.*, 1994; Ward *et al.*, 1995). Therefore, calnexin seems to lead it to the ERAD pathway. However, the role of calnexin in the ERAD remains controversial. Previous reports indicated that a diminished rate of physical dissociation of substrates from calnexin leads to ERAD in mammalian cells (Cabral *et al.*, 2000, 2001), suggesting that calnexin leads the substrate to ERAD. In contrast, inhibition of the interaction between calnexin and glycoproteins enhanced the degradation, indicating that calnexin prevents ERAD (Chen *et al.*, 1998; Wilson *et al.*, 2000).

In this study, we tried to clarify the role of calnexin in the ERAD of ΔF508 CFTR by using calnexin overexpression system. Our results showed that calnexin overexpression increased the ER retention of ΔF508 CFTR but partially attenuated the ERAD. Moreover, calnexin overexpression induced the formation of concentric membranous (CM) bodies of the ER where calnexin and ΔF508 CFTR accumulated. ΔF508 CFTR in CM bodies was not ubiquitinated, and calnexin overexpression inhibited formation of aggresomes and high molecular weight (HMW) complexes induced by a proteasomal inhibitor.

MATERIALS AND METHODS

Materials

The following antibodies were used in this study: mouse monoclonal anti-CFTR (C-terminus specific) (clone 24–1; Genzyme/Techne, Cambridge, MA), rabbit polyclonal anti-calnexin (C-terminus specific) (anti-CNX; SPA-860; Stressgen Biotechnologies, Victoria, BC, Canada), rabbit polyclonal anti-ubiquitin (anti-Ub; FL-76; Santa Cruz Biotechnology, Santa Cruz, CA), mouse monoclonal anti-ubiquitinated proteins (anti-Ub-Protein; clone FK2; Affiniti Bioreagents, Golden, CO), mouse monoclonal anti-20S proteasome subunit α7 (anti-20S; clone HC8; Affiniti Bioreagents), mouse monoclonal anti-vimentin (clone V9; Santa Cruz Biotechnology), mouse monoclonal anti-Hsp70 (clone C92F3A-5; Stressgen Biotechnologies), rat monoclonal anti-Hsc70 (clone 1B5; SPA-815; Stressgen Biotechnologies), rabbit polyclonal anti-calreticulin (anti-CRT; SPA-600; Stressgen Biotechnologies), mouse monoclonal anti-KDEL (anti-BiP; clone 10C3; Stressgen Biotechnologies), rabbit polyclonal anti-protein disulfide isomerase (PDI) (SPA-890; Stressgen Biotechnologies), mouse monoclonal anti-β-COP (clone maD; Sigma-Aldrich, St. Louis, MO), mouse monoclonal anti-KDEL receptor (anti-KDELr; clone KR-10; Stressgen Biotechnologies), mouse monoclonal anti-Golgi 58K protein (anti-p58; clone 58K-9; Sigma-Aldrich), mouse monoclonal anti-Lamp-1 (clone UH1; Developmental Studies Hybridoma Bank, University of Iowa, Iowa City, IA), and mouse monoclonal anti-FLAG M2 (Sigma-Aldrich) antibodies.

MG-132 and nocodazole were purchased from Calbiochem (San Diego, CA), and brefeldinA and cycloheximide were purchased from Sigma-Aldrich.

Cell Lines

Baby Hamster kidney (BHK) cells stably expressing green fluorescent protein (GFP)-CFTR (CFTR-BHK) and GFP-ΔF508 CFTR (ΔF508-BHK), and Chinese hamster ovary (CHO) cells stably expressing CFTR (CFTR-CHO) and ΔF508 CFTR (ΔF508-CHO) were grown and maintained as described previously (Lukacs *et al.*, 1994; Loo *et al.*, 1998). CFTR- and ΔF508-CHO cells were maintained in α-minimal essential medium (MEM) containing 7% fetal bovine serum, antibiotics, and 200 μM methotrexate. CFTR- and ΔF508-BHK cells were maintained in DMEM/F-12 medium containing 10% fetal bovine serum, antibiotics, and 500 μM methotrexate. CFBE41o⁻ and 16HBE14o⁻ cells were grown in MEM with 10% fetal bovine serum and antibiotics on glass-bottomed culture dishes coated with human fibronectin. To increase CFTR expression, cells were incubated with 1 mM (CFTR- and ΔF508-BHK cells) or 2 mM sodium butyrate (CFTR-, ΔF508-CHO, 16HBE14o⁻, and CFBE41o⁻ cells) for 20–24 h before analysis.

Recombinant Adenovirus

Recombinant adenovirus expressing human calnexin (Ad-CNX) or LacZ (Ad-LacZ) based on adenovirus 5 (Ad5) was produced as described previously (Okiyoneda *et al.*, 2002).

SDS-PAGE and Western Blotting

Subconfluent (90–100%) CFTR- and ΔF508-CHO cells grown on six-well plates were washed twice with ice-cold phosphate-buffered saline (PBS) and lysed at 4°C in 100 μl of radioimmunoprecipitation assay (RIPA) buffer (50 mM Tris-HCl, 150 mM NaCl, 1 mg/ml sodium deoxycholate, and 1% NP-40) containing 1% protease inhibitor cocktail (Sigma-Aldrich) and centrifuged at 15,000 × *g* for 10 min at 4°C. The supernatant was prepared as cell lysates (detergent-soluble fraction). To prepare the detergent-insoluble fraction, the precipitate was washed three times with RIPA buffer, solubilized in 40 μl of 10 mM Tris-HCl, 1% SDS for 10 min at room temperature (RT), and 160 μl of RIPA buffer, supplemented with protease inhibitor cocktail, was added (final concentration 1%). Insoluble fractions were passed several times through a 27-gauge needle to decrease the viscosity. The detergent-soluble and -insoluble fractions were subjected to SDS-PAGE on 6 or 7.5% polyacrylamide gels. Protein was electroblotted from the gels to polyvinylidene difluoride membrane. The membranes were blocked in 5% skim milk and 0.1% Tween 20 in PBS for 1 h at RT, and incubation with the primary antibodies specified in the figure legends was for 1 h at RT. The membranes were then washed three times in 0.05% Tween 20 in PBS and incubated with the appropriate secondary antibody for 1 h at RT. After washing, membranes were incubated with ECL detection reagents (Amersham Biosciences, Piscataway, NJ) and analyzed by luminescent image analyzer (LAS-1000; Fujifilm, Tokyo, Japan).

Pulse-Chase Analysis and Immunoprecipitation

Pulse-chase analysis and immunoprecipitation were carried out as described previously (Lukacs *et al.*, 1994). Subconfluent CFTR- and ΔF508-CHO cells infected with or without Ad-CNX were incubated for 30 min in methionine- and cysteine-free αMEM 48 h after infection, and then pulse-labeled for 20 min with 100 μCi/ml [³⁵S]methionine and [³⁵S]cysteine (>1000 Ci/mmol; Amersham Biosciences). For chasing, the cells were washed three times with PBS and the labeling medium was replaced by complete αMEM containing 1 mM cycloheximide. Radiolabeled CFTR was isolated by immunoprecipitation. The cells were washed with ice-cold PBS three times and then lysed at 4°C in 1 ml of RIPA buffer containing 1% protease inhibitor cocktail. Samples were centrifuged at 15,000 × *g* for 10 min at 4°C, and the supernatant was incubated for 2 h at 4°C with monoclonal anti-CFTR antibody immobilized in protein G Sepharose 4 Fast Flow (Amersham Biosciences). Immune complexes were precipitated, followed by four washes with 1 ml of RIPA buffer. Immunoprecipitated proteins were eluted for 15 min at 37°C with 2× concentrated loading buffer and analyzed on 6% SDS-PAGE gels. The gels were dried and analyzed with a BAS imaging plate scanner (BAS-2000; Fujifilm). The radioactivity associated with CFTR was quantified using Image Gauge software (version 3.4; Fujifilm).

Transfection

Transfection was performed using *Trans*IT-LT1 transfection reagents (Mirus, Madison, WI). Subconfluent cells grown on glass-bottomed culture dishes were transfected with 2 μg of plasmid DNA per dish.

Small Interfering RNA (siRNA) Preparation and Transfection

Specific siRNA was designed as described previously (Elbashir *et al.*, 2001). We used the 21-nucleotide (nt) sense strand (5′-GCAUCAUGCCAUCUCUG-CUdTdT, coding region 384–402 relative to the start codon) and the 21-nt antisense strand (5′-AGCAGAGAUGGCAUGAUGCdTdT) of calnexin mRNA (GenBank accession no. AB071869). siRNA duplex was prepared as described previously (Elbashir *et al.*, 2001). Transient transfection with siRNA was performed by using *Trans*IT-TKO (Mirus) as described by the manufacturer. siRNA duplex was used at a concentration of 10 nM.

Immunocytochemical Analysis and Confocal Laser Scanning Microscopy

Subconfluent cells grown on glass-bottomed culture dishes were washed twice with PBS, fixed in 3.7% paraformaldehyde in PBS for 20 min at RT, and permeabilized with 0.1% Triton-X in PBS for 20 min at RT. For immunostaining with anti-Golgi 58K protein or Lamp-1 antibodies, cells were permeabilized with 0.5% Triton-X in PBS or immunofluorescence buffer (150 mM NaCl, 5 mM NaN₃, 1 mM EDTA, 15 mM Tris-Cl, 0.1% gelatin, 0.01% saponin, pH 7.5) for 20 min at RT (Wimer-Mackin and Granger, 1996). All cells were washed twice with PBS, subsequently incubated in PBS containing 1% bovine serum albumin (BSA) (BSA/PBS) for 30 min at RT, and then incubated for 1 h with corresponding primary antibodies (1:100 dilution) in 1% BSA/PBS at RT. Cells were washed three times with PBS and then immunostained with fluorescein isothiocyanate- or tetramethylrhodamine B isothiocyanate (TRITC)-conjugated secondary antibodies (1:100 dilution; Jackson ImmunoResearch Laboratories, West Grove, PA) or Alexa Fluor 488-conjugated secondary antibody (1:100 dilution; Molecular Probes, Eugene, OR.) in 1% BSA/PBS for 45 min at RT. Cells were washed three times with PBS and mounted with Vectashield mounting medium (Vector Laboratories, Burlingame, CA). Cells were observed and analyzed with a Fluoview FV300 confocal laser scanning microscope (Olympus, Tokyo, Japan).
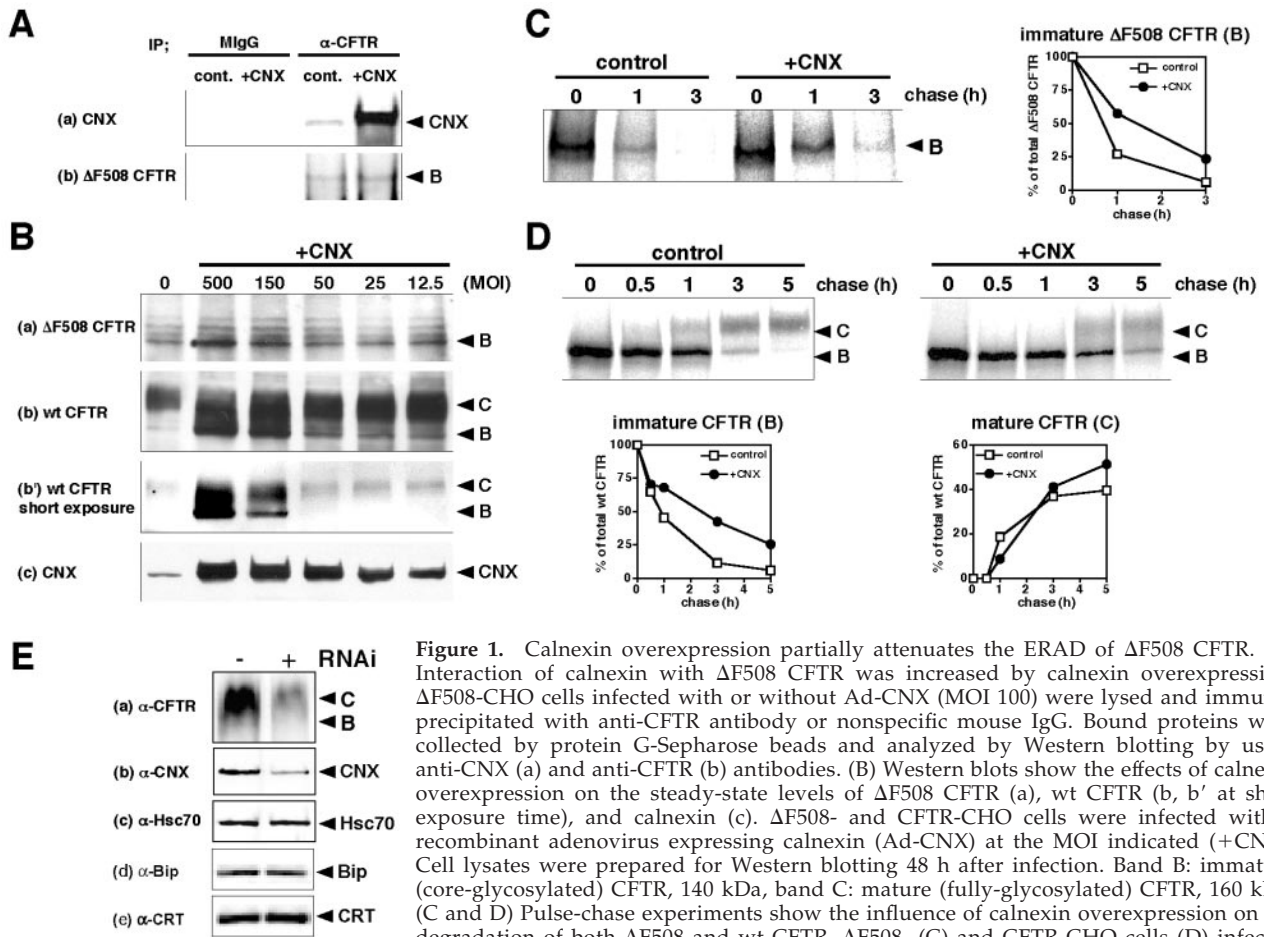
Figure 1. Calnexin overexpression partially attenuates the ERAD of ΔF508 CFTR. (A) Interaction of calnexin with ΔF508 CFTR was increased by calnexin overexpression. ΔF508-CHO cells infected with or without Ad-CNX (MOI 100) were lysed and immunoprecipitated with anti-CFTR antibody or nonspecific mouse IgG. Bound proteins were collected by protein G-Sepharose beads and analyzed by Western blotting by using anti-CNX (a) and anti-CFTR (b) antibodies. (B) Western blots show the effects of calnexin overexpression on the steady-state levels of ΔF508 CFTR (a), wt CFTR (b, b' at short exposure time), and calnexin (c). ΔF508- and CFTR-CHO cells were infected with a recombinant adenovirus expressing calnexin (Ad-CNX) at the MOI indicated (+CNX). Cell lysates were prepared for Western blotting 48 h after infection. Band B: immature (core-glycosylated) CFTR, 140 kDa, band C: mature (fully-glycosylated) CFTR, 160 kDa. (C and D) Pulse-chase experiments show the influence of calnexin overexpression on the degradation of both ΔF508 and wt CFTR. ΔF508- (C) and CFTR-CHO cells (D) infected with or without Ad-CNX (+CNX, MOI 100 [C] or 50 [D]) were pulse labeled 48 h after infection. Radiolabeled CFTR was isolated from cell lysates after the indicated chase period by immunoprecipitation with anti-CFTR antibody and analyzed by SDS-PAGE. The right panel in C and the lower panels in D show the quantification of pulse-chase experiments in ΔF508- and CFTR-CHO cells, respectively. The intensity of the band indicating ΔF508 CFTR and wt CFTR was quantified by Image Gauge software (version 3.4; Fujifilm) and expressed as a percentage of the total material present at $t = 0$, respectively. The data shown are representative of three independent experiments. (E) Effect of calnexin-specific RNAi on the steady-state level of wt CFTR. Cell lysates from CFTR-CHO cells transfected with or without calnexin-specific siRNA (10 nM) were subjected to Western blotting with anti-CFTR (a), -calnexin (b), -hsc70 (c), -Bip (e), and -calreticulin (f) antibodies 48 h after transfection.

Fluorescence Recovery after Photobleaching (FRAP) Analysis

ΔF508-BHK cells infected with Ad-CNX were washed twice with PBS and the culture medium was replaced with CO_2-independent medium (Invitrogen, Carlsbad, CA) containing 1 mM cycloheximide, either immediately or after fixation, in 3.7% paraformaldehyde in PBS for 20 min at RT. The temperature was maintained at 37°C. FRAP analysis was carried out on a FV300 confocal laser scanning microscope with a 60×, 1.25 numerical aperture objective (Olympus). A single z-section was imaged before and at 5- to 7.5-s intervals after photobleaching. The photobleaching was carried out at a wavelength of 488 nm at maximal power for iterations. The fluorescence intensities of the photobleached region were obtained using Fluoview software (version 3.3), and data were analyzed using Microsoft Excel.

Transmission Electron Microscopy

ΔF508-BHK cells infected with or without Ad-CNX were fixed in 1.0% glutaraldehyde for 30 min and postfixed in 1.0% osmium tetroxide for 30 min at 4°C. After dehydration in a graded ethanol series, the cells were embedded in epoxy resin. Ultrathin sections stained with uranyl acetate and lead citrate were observed with an H-7500 electron microscope (Hitachi, Tokyo, Japan).

RESULTS

Calnexin Overexpression Partially Attenuates the ERAD of ΔF508 CFTR

Previous reports have indicated that calnexin may target ΔF508 CFTR to the ERAD, but contradictory findings have been reported. To clarify the role of calnexin on the fate of ΔF508 CFTR, we examined the effect of calnexin overexpression. By coimmunoprecipitation using anti-CFTR antibody, we showed that calnexin overexpression increased the interaction between calnexin and ΔF508 CFTR (Figure 1A). If calnexin can promote the ERAD, calnexin overexpression would lead to a diminished expression of ΔF508 CFTR; however, by Western blot analysis of CHO cells stably expressing ΔF508 CFTR (ΔF508-CHO) we observed that calnexin overexpression increased the steady-state level of immature ΔF508 CFTR in a multiplicity of infection (MOI)-dependent manner (Figure 1B, a). Similarly, calnexin overexpression increased the steady-state level of both immature (band B) and mature (band C) wt CFTR in a MOI-dependent man-
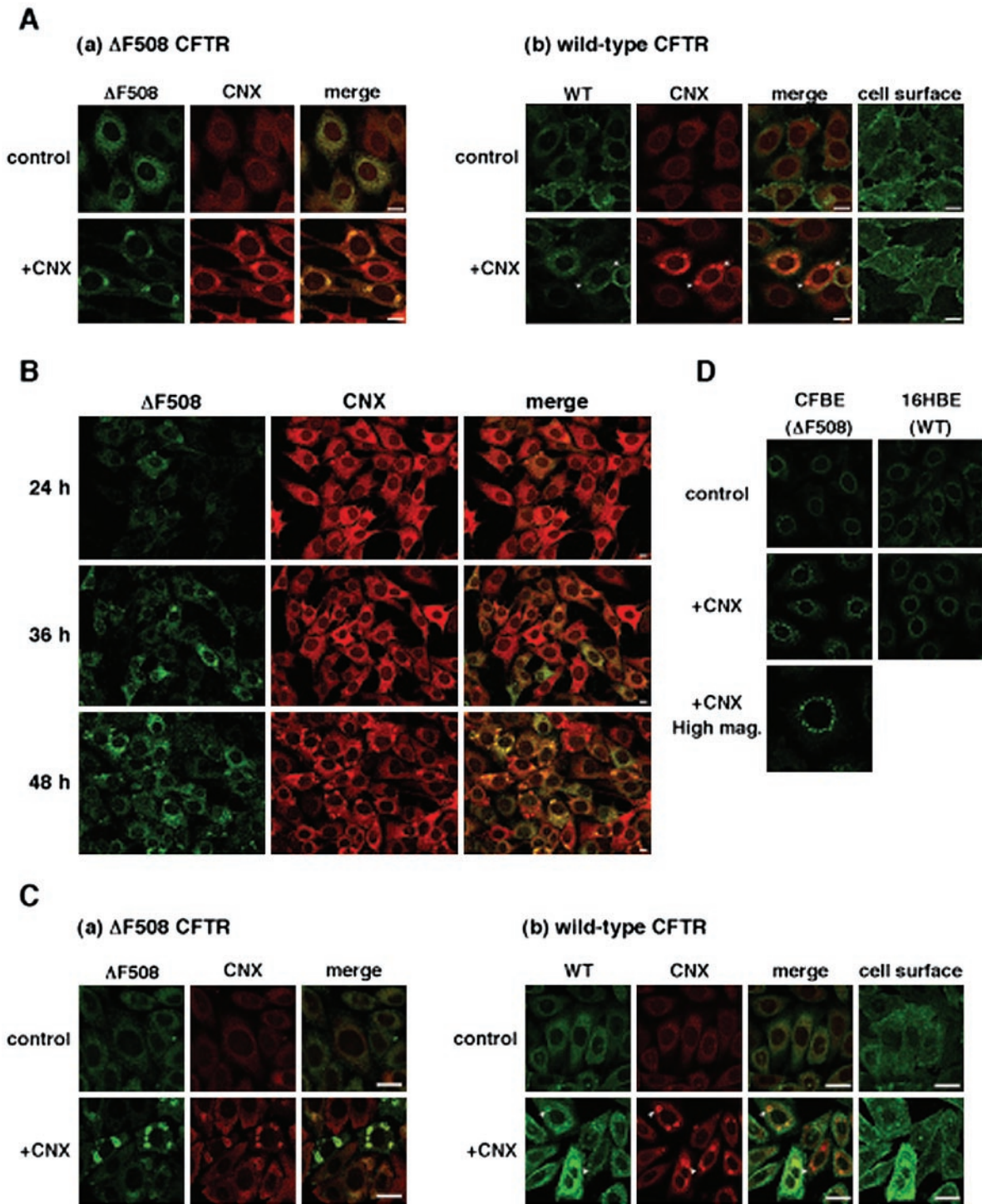
Figure 2. Calnexin overexpression formed IB-like structures where ΔF508 CFTR and calnexin accumulated. (A) All panels are fluorescence micrographs of BHK cells stably expressing ΔF508 CFTR-GFP (a, ΔF508-BHK) and wt CFTR-GFP (b, CFTR-BHK). The cells were infected with or without Ad-CNX at a MOI 50 (+CNX), and 48 h after infection cells were fixed and permeabilized, immunostained with anti-calnexin antibody, and visualized with TRITC-conjugated secondary antibody. Analysis was performed by confocal laser scanning microscopy. GFP fluorescence is shown in the left panels (a, ΔF508 CFTR; b, wt CFTR), TRITC fluorescence in the middle panels (CNX), and right panels show the overlay (merge). Note that calnexin overexpression formed IB-like structures and ΔF508 CFTR specifically accumulated in the structures. Arrowheads represent the regions in which wt CFTR slightly accumulated with calnexin. (B) Time course of IB-like structure formation. ΔF508-BHK cells were infected with Ad-CNX (MOI 50) and incubated for the times indicated. Note that formation of IB-like structures of ΔF508 CFTR coincides with that of calnexin. (C) ΔF508- (a) and CFTR-CHO (b) cells were infected with or without Ad-CNX (MOI 50) and 48 h after infection cells were fixed and permeabilized, immunostained with anti-CFTR and anti-calnexin antibodies, and visualized with fluorescein isothiocyanate- and TRITC-conjugated secondary antibodies. (D) CFBE41o⁻ cells (ΔF508 CFTR) and 16HBE14o⁻ (wt CFTR) were infected with or without Ad-CNX (MOI 50), and 48 h after infection cells were fixed and permeabilized, immunostained with anti-CFTR antibody, and visualized with Alexa Flour488-conjugated secondary antibody. The cells were imaged so that the ER region was in focus, except for some images that were focused on the cell surface (cell surface). Bars, 10 μm.
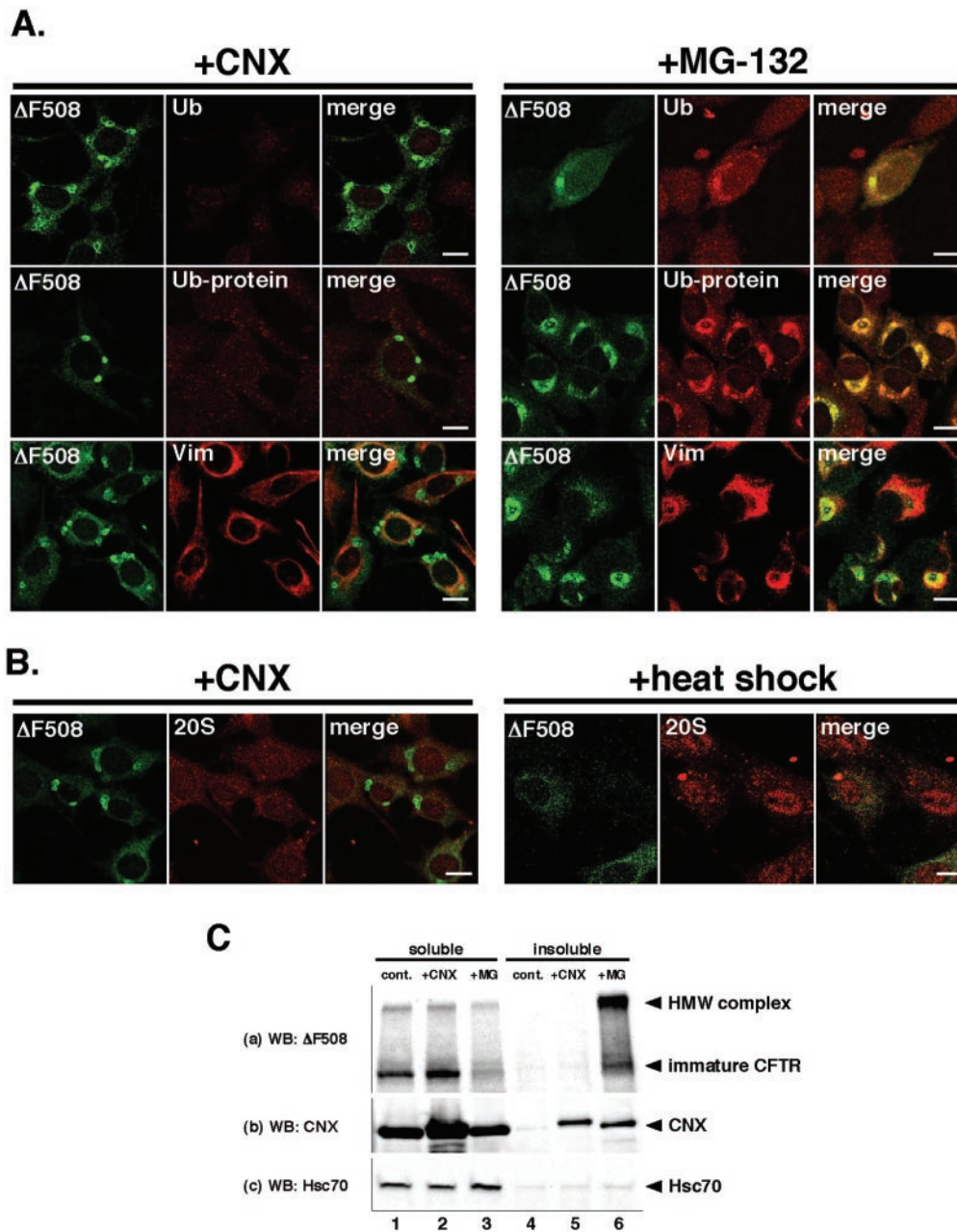
Figure 3. IB-like structures are not aggresomes. (A and B) Fluorescence micrographs of ΔF508-BHK cells infected with Ad-CNX at a MOI 50 (+CNX) or treated with 10 μM MG-132 (+MG-132) for 6 h. The cells were immunostained with anti-ubiquitin (Ub), anti-ubiquitinated protein (Ub-protein), anti-20S proteasome (20S), and anti-vimentin (Vim) antibodies, and visualized with TRITC-conjugated secondary antibodies. When 20S proteasome was immunostained, aggresomes were formed by heat shock (+heat shock, 42°C for 2 h and subsequently incubated at 37°C for 5 h). Note that aggresomes formed by MG-132 or heat shock are positive for aggresome markers, whereas IB-like structures formed by calnexin overexpression are negative. Bar, 10 μm. (C) Detergent solubility of IB-like structures. ΔF508-CHO cells were infected with Ad-CNX (MOI 50, CNX, lanes 2 and 5) or treated with MG-132 (2 μM, MG, lanes 3 and 6) for 24 h. Detergent-soluble (lanes 1–3) and -insoluble fractions (lanes 4–6) prepared from the cells were analyzed by Western blotting with anti-CFTR (a), anti-calnexin (b), and anti-Hsc70 antibodies (c). Note that calnexin overexpression increased the amount of the detergent-soluble ΔF508 CFTR.

ner (Figure 1B, b and b'). To further support these observations, pulse-chase analysis revealed that calnexin overexpression partially attenuated the degradation of immature ΔF508 CFTR and prolonged the half-life ($t_{1/2}$) about twofold (control, $t_{1/2}$ ~45 min; CNX, $t_{1/2}$ ~90 min) (Figure 1C). Similarly, calnexin overexpression moderately attenuated the ERAD of wt CFTR and prolonged the $t_{1/2}$ about threefold (control, $t_{1/2}$ ~45 min; CNX, $t_{1/2}$

~130 min) (Figure 1D, immature CFTR). The reason why wt CFTR at the steady-state level is increased by CNX overexpression (Figure 1B) is maybe because wt CFTR is temporarily retained by calnexin in the ER and then goes to the cell surface through the Golgi. It is likely that the results of calnexin overexpression may partly reflect the physiological condition, because down-regulation of endogenous calnexin by using siRNA decreased the CFTR
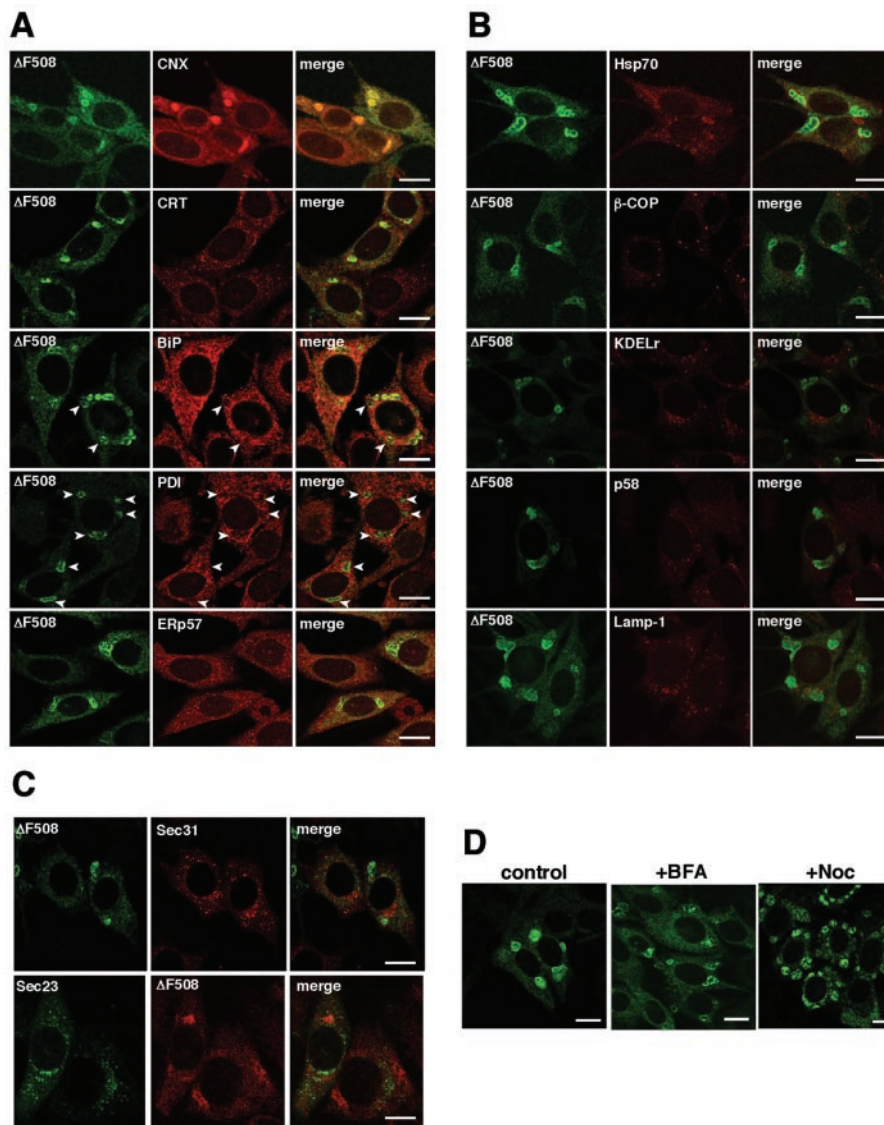
Figure 4. IB-like structures are concentric membranous bodies of the ER. (A and B) Cellular localization of IB-like structures in comparison with ER and other organelle markers. All panels are fluorescence micrographs of ΔF508-BHK cells infected with Ad-CNX (MOI 50). Forty-eight hours after infection, cells were immunostained with anti-calnexin (CNX), anti-calreticulin (CRT), anti-BiP, anti-PDI, and anti-ERp57 antibodies (A), or with anti-Hsp70, anti-β-COP, anti-KDEL receptor (KDELr), anti-Golgi 58K protein (p58), and anti-Lamp-1 (B), and visualized with TRITC-conjugated secondary antibodies. Note that ΔF508 CFTR mainly clustered in regions devoid of BiP and PDI immunostaining (arrowhead). (C) IB-like structures are not located at ER exit sites. ΔF508-BHK or -CHO cells were infected with Ad-CNX (MOI 50) and transfected with Sec31-FLAG or Sec23-GFP. Forty-eight hours after transfection, cells were immunostained with anti-FLAG or anti-CFTR antibodies, and visualized with TRITC-conjugated secondary antibodies. (D) Formation of IB-like structures is brefeldin A insensitive and microtubule dependent. ΔF508-BHK cells were infected with Ad-CNX (MOI: 50), and 48 h after infection the cells were treated with 5 μg/ml brefeldin A for 5 h (+BFA) or with 10 μg/ml nocodazole for 5 h (+Noc) before analysis. Bar, 10 μm. (E–H) Transmission electron microscopy of ΔF508-BHK cells infected with (E, G, and H) or without (F) Ad-CNX at a MOI 50. (G) Higher magnification view of the section indicated by a black box in E. (H) Higher magnification view of a section from an infected cell. N, nucleus. Bars, 1 μm. (I) FRAP analysis was performed in ΔF508-BHK cells infected with Ad-CNX (MOI 50). Images are shown before photobleaching (prebleach), with the bleached spot indicated by an arrowhead, and at the indicated times after the photobleaching. After photobleaching, cells were incubated with 1 mM cycloheximide at 37°C and observed at 7.5-s intervals for 750 s. (J) Quantification of FRAP analyses in ΔF508-BHK cells infected with Ad-CNX (MOI 50). Fluorescence intensities (normalized to prebleach value) from FRAP analyses are plotted against time for ΔF508-GFP in the IB-like structure of fixed cells (open circles) and living cells (close circles). Fluorescence was recovered immediately after photobleaching in living cells and the IB-like structure reformed.

expression without affecting the expression of hsc70, Bip, and calreticulin (Figure 1E). siRNA of calreticulin rather increased the CFTR expression without affecting the expression of calnexin, hsc70, and Bip in the present study (our unpublished data).

Calnexin Overexpression Induces the Formation of Inclusion Body (IB)-like Structures in Which ΔF508 CFTR Accumulates

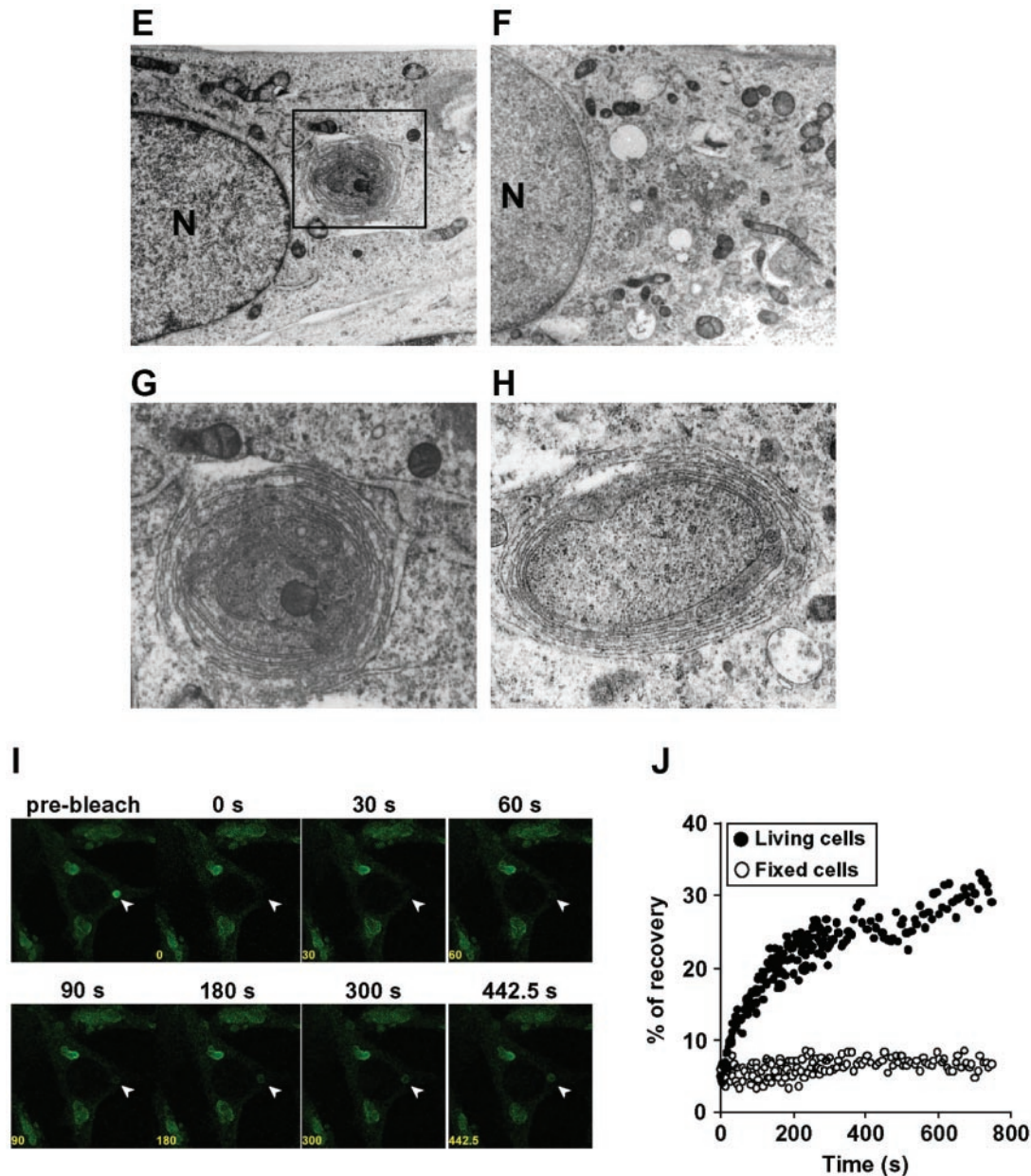To examine the effect of calnexin overexpression on the cellular localization of ΔF508 CFTR, immunocytochemical

Figure 4. (continued from facing page).

analyses by using a confocal laser scanning microscope were performed in BHK cells stably expressing GFP-ΔF508 (ΔF508-BHK) or GFP-wt CFTR (CFTR-BHK). In agreement with a previous report (Loo *et al.*, 1998), ΔF508 CFTR was located in the ER with calnexin (Figure 2A, a), whereas most wt CFTR was located on the cell surface in the steady state (Figure 2A, b). When calnexin was overexpressed, it formed IB-like structures in both CFTR- and ΔF508-BHK cells (Figure 2A, +CNX). Formation of IB-like structures was MOI-dependent (our unpublished data), and in many cases the structures emerged near the nucleus as a ring-shape. Interestingly, ΔF508 CFTR significantly accumulated in IB-like structures with calnexin (Figure 2A, a; +CNX). In contrast, most wt CFTR was dispersed in the cells and expressed at the cell surface, although a small amount of wt CFTR also

accumulated in IB-like structures (Figure 2A, b; +CNX, arrowhead).

We next examined the time course of IB-like structure formation after calnexin overexpression in ΔF508-BHK cells. IB-like structures had not emerged 24 h after infection but some occurred at 36 h (Figure 2B). Calnexin and ΔF508 CFTR simultaneously accumulated in IB-like structures (Figure 2B), indicating that calnexin participates in ΔF508 CFTR accumulation. To exclude the possibility that IB-like structure formation is an artifact of using GFP-tagged proteins, we performed double immunofluorescence staining with anti-CFTR and anti-calnexin antibodies in CFTR- and ΔF508-CHO cells. Similar results were obtained in these cells (Figure 2C). Moreover, calnexin overexpression formed IB-like structures in the cells in which neither CFTRs were ex-

pressed (our unpublished data), indicating that their formation is CFTR independent.

Finally, we determined whether calnexin overexpression induces the formation of IB-like structures in a human cystic fibrosis airway epithelial cell line, CFBE41o⁻ (Zeitlin *et al.*, 1991), that endogenously expresses ΔF508 CFTR. Although the pattern of IB-like structures was slightly different in CFBE41o⁻ cells, calnexin overexpression induced the ΔF508 CFTR accumulation in structures around the nucleus in these cells, but not in a human airway epithelial cell line, 16HBE14o⁻ (Cozens *et al.*, 1994), that endogenously expressed wt CFTR (Figure 2D).

IB-like Structures Are Not Aggresomes

It has been reported that inhibition of proteasomal degradation leads to misfolded CFTR accumulation in the cytosol and aggresome formation (Johnston *et al.*, 1998). Aggresomes consist of aggregated proteins, such as polyubiquitinated proteins, proteasomes, and Hsp70, and are surrounded by vimentin cages (Johnston *et al.*, 1998; Wigley *et al.*, 1999). Therefore, we tried to determine whether the IB-like structures are aggresomes. Immunocytochemical analysis showed that aggresome marker proteins such as ubiquitin, ubiquitinated proteins, and 20S proteasome did not accumulate in IB-like structures (Figure 3, A and B, +CNX). In contrast, aggresome markers accumulated in aggresomes formed by the proteasome inhibitor MG-132 (Figure 3A, +MG-132). Although 20S proteasome was not detected in aggresomes induced by MG-132 (our unpublished data), it was detected in aggresomes induced by heat shock (Figure 3B, +heat shock). Unlike aggresomes, IB-like structures were not surrounded by vimentin cages (Figure 3A).

To further discriminate between IB-like structures and aggresomes, we examined the detergent solubility of IB-like structures in ΔF508-CHO cells. In cells treated with MG-132, most ΔF508 CFTR was detected in the detergent-insoluble fraction, along with calnexin, as a HMW complex, indicating polyubiquitinated ΔF508 CFTR (Jensen *et al.*, 1995; Xiong *et al.*, 1999; Fuller and Cuthbert, 2000) (Figure 3C, lanes 3 and 6). In contrast, in cells infected with Ad-CNX, no ΔF508 CFTR was detected in the detergent-insoluble fraction, although a smaller amount of calnexin was detected (Figure 3C, lanes 2 and 4). Rather, ΔF508 CFTR was detected mainly as a core-glycosylated form in the detergent-soluble fraction (Figure 3C, lane 2), indicating that IB-like structures consisted of detergent-soluble immature ΔF508 CFTR. Therefore, IB-like structures induced by calnexin overexpression were not aggresomes.

IB-like Structures Are Concentric Membranous Bodies of the ER

To determine the cellular localization of the IB-like structures, we performed immunostaining with antibodies against several organelle markers. ER chaperones such as calreticulin and ERp57 were partially colocalized with ΔF508 CFTR in IB-like structures (Figure 4A). The ER–Golgi complex intermediate compartment (ERGIC) and *cis*-Golgi markers β-COP, KDEL receptor, and rodent ERGIC-53; Golgi 58K protein (p58); a lysosome marker, Lamp-1; and a cytosolic marker, Hsp70, were not found in IB-like structures (Figure 4B), indicating that they were in the ER. Interestingly, ΔF508 CFTR was mainly clustered in regions devoid of BiP and PDI (Figure 4, A and B, arrowhead). We further examined whether the ER exit sites (Antonny and Schekman, 2001; Mezzacasa and Helenius,

2002; Yoo *et al.*, 2002) locate in IB-like structures by using Sec23-GFP or Sec31-FLAG expression vectors because antibodies against the components of COPII-coated vesicles, such as Sec23, were not available for immunofluorescence studies. Immunocytochemical analyses showed that the ΔF508 CFTR in IB-like structures was not colocalized with COP II components (Figure 4C), indicating that ER exit sites are not located in IB-like structures. It has been reported that ERAD inhibition leads to accumulation of ERAD substrates, such as asialoglycoprotein receptor H2a, in the ER quality control (ERQC) compartment (Kamhi *et al.*, 2001). Formation of the ERQC compartment is brefeldin A (BFA) insensitive and microtubule dependent (Kamhi *et al.*, 2001). Similar to the ERQC compartment, IB-like structure formation was BFA insensitive and nocodazole, a microtubule polymerization inhibitor, partially dispersed IB-like structures in cells (Figure 4D).

We used transmission electron microscopy to resolve the ultrastructure of the IB-like structures. In ΔF508-BHK cells infected with Ad-CNX, a concentric arrangement of membranes occurred near the nucleus (Figure 4E, box), although it never occurred in noninfected cells (Figure 4F). This concentric arrangement of membranes seemed to be connected to the peripheral ER, and these membranes enclosed cytoplasmic components such as ribosomes, polysomes, lipid, and mitochondria (Figure 4, G and H). Thus, the concentric membranes seemed to form a CM body of the ER (Ghadially, 1996). CM bodies of the ER differed from structures in which ER soluble and membrane proteins accumulated, such as the Russel body (Kopito and Sitia, 2000) and crystalloid ER (Yamamoto *et al.*, 1996). In this study, we found that one or two CM bodies of the ER occurred in cells infected with Ad-CNX. However, their formation was not due to an artifact of recombinant adenovirus infection, because we did not find the structures in cells infected with adenovirus expressing calreticulin or β-galactosidase (our unpublished data). Moreover, the CM bodies were formed by calnexin overexpression by using cationic liposomes (our unpublished data). In immunocytochemical studies, IB-like structures formed by calnexin overexpression were seen as ring-shaped structures (Figure 2A) that were consistent with the morphological features of CM bodies of the ER.

To further characterize CM bodies of the ER, we performed FRAP analysis. ΔF508-BHK cells were infected with Ad-CNX at MOI 50 to form CM bodies. About 48 h after infection, a CM body (indicated by arrowhead) was photobleached by laser pulses, and fluorescence recovery was recorded by serial imaging after 1 mM cycloheximide treatment. In living cells, the fluorescence of a photobleached CM body was progressively recovered immediately after photobleaching, and CM bodies were recreated in the same place (Figure 4I). In contrast, fluorescence recovery did not occur in fixed cells (our unpublished data). Quantification analysis of FRAP showed that ~30% of the fluorescence in the CM body was recovered 10 min after photobleaching in living cells (Figure 4J). These results indicate that fluorescence recovery resulted from the lateral diffusion of ΔF508 CFTR-GFP localized in the ER. Therefore, CM bodies of the ER are dynamic and connected to the peripheral ER reticular domain.

Calnexin Overexpression Attenuates Aggresome Formation

Calnexin overexpression partially attenuated the ERAD of ΔF508 CFTR, leading to accumulation of ΔF508 CFTR in CM bodies of the ER. Moreover, the accumulated ΔF508 CFTR was not ubiquitinated. To confirm the possibility that calnexin overexpression attenuates aggresome forma-
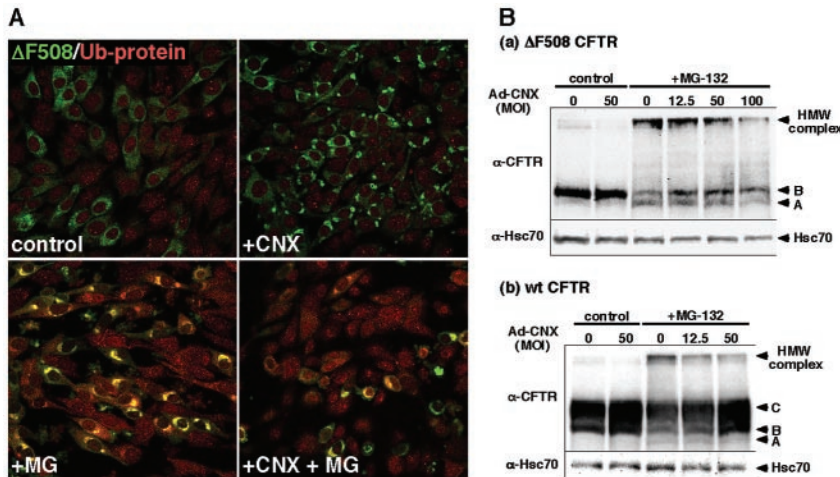
Figure 5. Calnexin overexpression moderately attenuates aggresome formation. (A) Fluorescence micrographs of ΔF508-BHK cells infected with or without Ad-CNX at MOI 50. Forty-eight hours after infection, cells were treated with 10 μM MG-132 for 6 h. Cells were immunostained with anti-ubiquitinated proteins (Ub-proteins) antibody and visualized with TRITC-conjugated secondary antibodies. Merged images show that calnexin overexpression inhibits aggresome formation. (B) Calnexin overexpression attenuates the formation of HMW complex of both wt and ΔF508 CFTR. ΔF508-CHO cells (a) and CFTR-CHO cells (b) infected with or without Ad-CNX at an MOI indicated were treated with 10 μM MG-132 for 3 h. Cell lysates were prepared for Western blotting with anti-CFTR and -Hsc70 antibodies. Hsc70 is used as the loading control. Band A, immature (unglycosylated) CFTR, 130 kDa. Band B, immature (core-glycosylated) CFTR, 140 kDa. Band C, mature (fully glycosylated) CFTR, 160 kDa.

tion, we examined the effect of calnexin overexpression on aggresome formation induced by MG-132. In ΔF508-BHK cells treated with MG-132 (10 μM), many aggresomes accumulating ubiquitinated ΔF508 CFTR were formed (Figure 5A). Aggresome formation by MG-132 was moderately decreased by calnexin overexpression (Figure 5A). In control, aggresomes were detected in ~49% of the total cells, whereas with calnexin overexpression only 7.5% of the cells had aggresome formation (Figure 5A, bottom). Because the ΔF508 CFTR accumulating in CM bodies was not ubiquitinated (Figure 3A), calnexin overexpression may inhibit the ubiquitination and retrotranslocation of ΔF508 CFTR. Indeed, Western blots show that calnexin overexpression attenuated the formation of HMW complex of both wt and ΔF508 CFTR induced by MG-132 in a MOI-dependent manner (Figure 5B), indicating that calnexin overexpression inhibits ubiquitination. It is well known that when misfolded proteins accumulate in the ER, ER chaperones' expression is induced by unfolded protein response (Kaufman, 1999). However, ER chaperones BiP and GRP94 were not increased in both ΔF508-CHO and ΔF508-BHK cells infected with Ad-CNX (our unpublished data). Rather, BiP and GRP94 were slightly decreased by calnexin overexpression (our unpublished data). This result may explain the fact that CFTR does not interact with BiP (Pind *et al.*, 1994).

CM Bodies of the ER Are Functional Compartments

One of the ways to establish that CM bodies are functional is to prove that they are connected to the late secretory pathway. Wild-type CFTR, but not ΔF508 CFTR, could leave the CM bodies for the late secretory pathway. We tried to visualize the transport of wt CFTR from CM bodies to the Golgi complex. To retain wt CFTR in CM bodies, we treated the cells with BFA, an inhibitor of ER–Golgi transport. In BFA-treated cells, the ER–Golgi transport of wt CFTR was inhibited and wt CFTR accumulated in the ER (Figure 6A, control). When calnexin was overexpressed in BFA-treated cells, wt CFTR accumulated with calnexin in the CM bodies (Figure 6A, +CNX). It is likely that colocalization of wt CFTR with calnexin in CM body is not due to wt CFTR misfolding because BFA treatment does not affect the conformation (Lukacs *et al.*, 1994; Chen et al., 2000). Similar to the CM bodies in which ΔF508 CFTR accumulated (Figure 6D),

many CM bodies were detected at least 3 h after cycloheximide treatment (Figure 6A, +CHX), indicating that at least a portion of them was composed of ER-retained wt CFTR. Then, we monitored the trafficking of accumulated wt CFTR after BFA washout. Before BFA washout, wt CFTR was localized with calnexin in the CM bodies (Figure 6B, 0 h). After BFA washout, wt CFTR left the CM bodies and accumulated in spot-like structures, probably the ER exit sites (Figure 6C, 420 s). The spot-like structures congregated and formed intermediate carriers, probably ERGIC, and these carriers moved toward the juxtanuclear region (Figure 6C, 1980 s). About 1 h after BFA washout, wt CFTR left the CM bodies to the juxtanuclear region where KDEL receptor was partially localized (our unpublished data), indicating that wt CFTR was localized in the Golgi complex (Figure 6B, 1 h). After 3 h, most wt CFTR had reached the cell surface (Figure 6B, 3 h), indicating that the wt CFTR in CM bodies transited to the late secretory pathway.

DISCUSSION

Calnexin is an ER chaperone that has a central role in the ER quality control. Although it has been thought that calnexin specifically retains misfolded proteins in the ER, leading them to the ERAD, the role of calnexin in the ERAD was controversial. In this study, we showed that calnexin overexpression partially attenuated the ERAD of misfolded CFTR and accumulated it in CM body of the ER. It is unlikely that formation of CM bodies is necessary for attenuation of the ERAD because calnexin overexpression at a low MOI (e.g., 12.5) in which there are few CM bodies, increased the steady-state level of ΔF508 CFTR (Figure 1A). ΔF508 CFTR in CM body was not ubiquitinated (Figure 3), and calnexin overexpression moderately attenuated the formation of aggresomes and HMW complexes induced by MG-132 (Figure 5B), indicating that interaction with calnexin might inhibit the ubiquitination and retrotranslocation of ΔF508 CFTR. Therefore, calnexin retains misfolded CFTR in the ER but does not lead it to the ERAD pathway. Other key molecules for ERAD such as ubiquitin ligases and Man$_8$-lectin (Hosokawa *et al.*, 2001; Meacham *et al.*, 2001; Lenk *et al.*, 2002; Molinari *et al.*, 2002; Yoshida *et al.*, 2002) seem to participate in the ERAD targeting of ΔF508 CFTR after dissociation from calnexin. It has been reported that after dis-
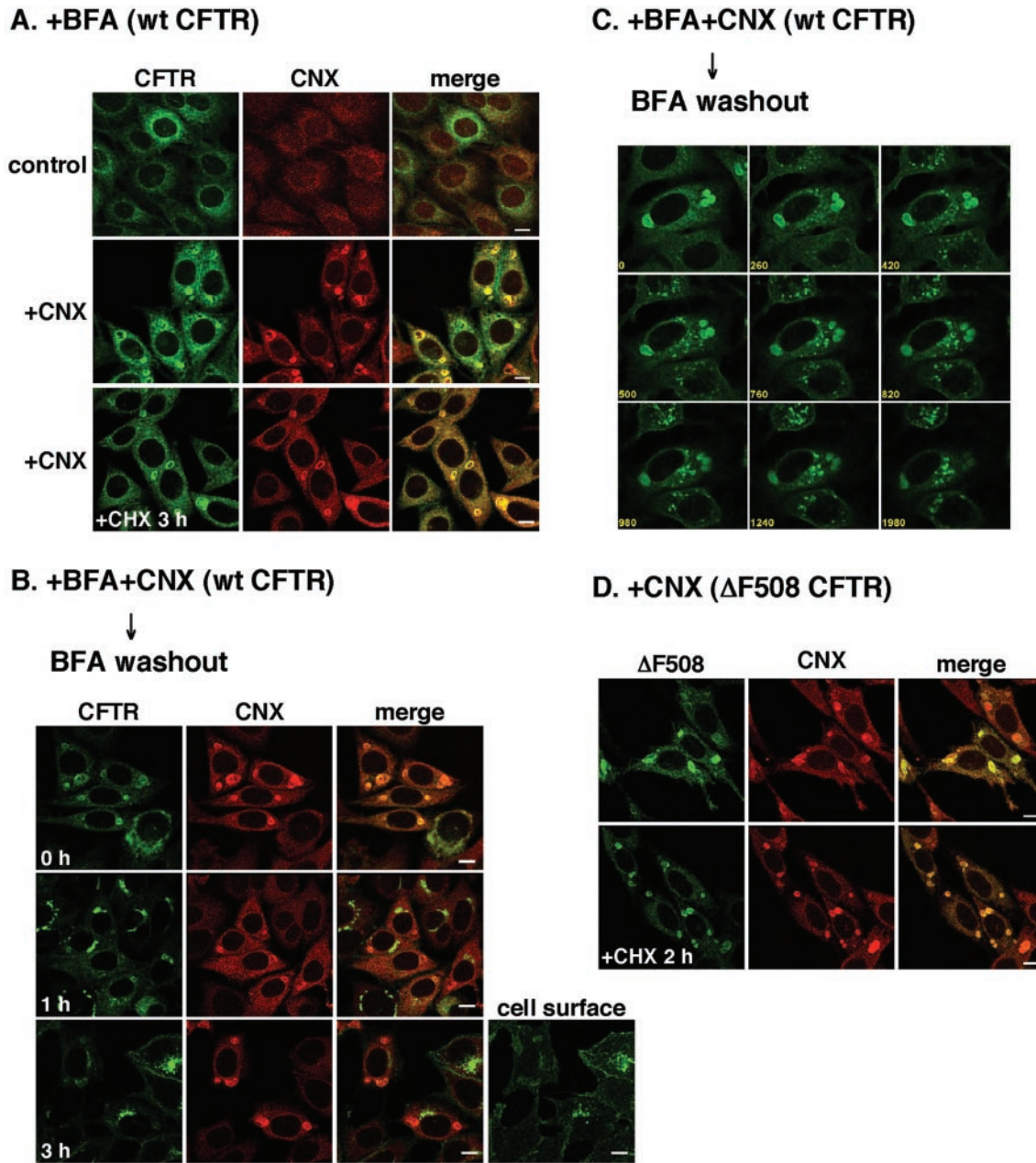
Figure 6. Concentric membranous body of the ER is connected to the late secretory pathway. (A) BFA treatment caused the accumulation of wt CFTR in CM bodies upon calnexin overexpression. CFTR-BHK cells infected with or without Ad-CNX (MOI 50) were treated with 5 µg/ml BFA for 6 h after 42 h after infection. Before fixation, cells were continuously treated with 1 mM cycloheximide for 3 h upon BFA treatment (A, +CHX). After fixing, cells were immunostained with anti-calnexin antibody and visualized with TRITC-conjugated secondary antibody. (B and C) Transport of wt CFTR from the CM bodies after BFA washout. (B) After BFA treatment for 6 h, cells were incubated with medium containing with 1 mM cycloheximide (BFA washout), fixed, and immunostained with anti-calnexin antibody. (C) After BFA washout, living cells were observed at 20-s intervals, for 33 min, at 37°C. The numbers in the panels show the incubation time periods (seconds) after BFA washout. (D) ΔF508 CFTR was retained in CM bodies. ΔF508-BHK cells infected with Ad-CNX (MOI 50) were treated with 1 mM cycloheximide for 2 h before fixation (+CHX). The cells were imaged so that the ER region was in focus, except for one image that focused on the cell surface (B, cell surface). Bar, 10 µm.

sociation from calnexin, BiP, and PDI are mainly involved in determining the direction of ERAD substrates toward retrotranslocation and ERAD (Cabral *et al.*, 2002; Molinari *et al.*, 2002). Our finding that CM bodies of the ER localize in ER regions devoid of BiP and PDI (Figure 4) may partly explain one of the mechanisms by which calnexin overexpression attenuated ERAD.

Furthermore, assuming that CM body formation excludes other ER lumenal proteins as well, it is predicted that further processing of oligosaccharides in the mutant CFTR should be arrested as long as it is sequestered in the CM bodies. This would prolong "off-time" duration of the CFTR from the reglucosylation-mediated calnexin cycle (Parodi, 2000; Cabral *et al.*, 2001; Schrag *et al.*, 2003)

and likely delay its mannose trimming to Man8B-containing oligosaccharides, which is known to trigger ERAD (Jakob *et al.*, 1998). Recently (during preparing this manuscript), it has been reported that Edem, a putative Man$_8$-lectin, functions as an acceptor of terminally misfolded glycoproteins released from calnexin (Molinari *et al.*, 2003; Oda *et al.*, 2003). Similar to other ERAD substrates, Edem may lead ΔF508 CFTR to the ERAD pathway after release from CM bodies. Hence, we think that CM bodies may function as a certain type of kinetic trap for ΔF508 CFTR, thus rendering it either more chance to fold in the calnexin complex or making a pause for disposal. As a result, ERAD efficiency seems to be reduced when calnexin is overexpressed. Similarly, this may explain why formation of CM bodies delayed ER exit of wt CFTR (Figure 1D). In either case, release of CFTR from CM bodies could occur at the off-phase of the equilibrium when glucosidase II "fixes" the status by deglucosylating the dissociated monoglucosylated CFTR (Zapun *et al.*, 1997). Alternatively, one could argue that CFTR may be trapped in the CM body in a nonglycan-mediated manner (Ihara *et al.*, 1999; Saito *et al.*, 1999; Danilczyk and Williams, 2001). In this model, misfolded moiety of CFTR should be responsible for the association. Currently, we were unable to exclude the possibility, however, we think it unlikely because 1) CM body is a dynamic structure (Figures 4, I and J, and 6) so that once-bound CFTR should be dissociated from the CM body; and 2) no cellular factor has been identified to release the substrate from calnexin other than glucosidase II, despite the extensive studies on the ER quality control (Ellgaard and Helenius, 2003; Schrag *et al.*, 2003).

It is interesting why calnexin overexpression formed the CM bodies of the ER (Figure 4). CM bodies of the ER are usually composed of paired membrane arrays (Ghadially, 1996). Sequestered at the center of the concentric profiles of such bodies lie a portion of the cell cytoplasm, often containing organelles and inclusions, typically lipid droplets and mitochondria (Ghadially, 1996). It has been known that normal cells such as cerebellar Purkinje cells and pathologically altered cells have CM bodies in their cytoplasm (Takei *et al.*, 1994; Ghadially, 1996). Moreover, it is thought that formation of CM bodies may represent an adaptive response to nonphysiological conditions such as hypoxia (Takei *et al.*, 1994). CM bodies were also induced by overexpression of inositol 1,4,5-trisphosphate receptor, an ER membrane protein (Takei *et al.*, 1994). Thus, overexpression of an ER membrane protein may induce formation of CM bodies. However, we think that calnexin may be directly involved in formation of CM bodies because overexpression of ER membrane proteins, such as inositol 1,4,5-trisphosphate receptor that interacts with calnexin, induces formation of CM bodies. In contrast, overexpression of other ER membrane proteins, such as microsomal aldehyde dehydrogenase that is not known to interact with calnexin, formed crystalloid ER but not CM bodies (Yamamoto *et al.*, 1996). In terms of the function, it may be reasonable to think that calnexin is directly involved in the formation of CM bodies.

REFERENCES

Anderson, M.P., Berger, H.A., Rich, D.P., Gregory, R.J., Smith, A.E., and Welsh, M.J. (1991). Nucleoside triphosphates are required to open the CFTR chloride channel. Cell *67*, 775–784.

Antonny, B., and Schekman, R. (2001). ER export: public transportation by the COPII coach. Curr. Opin. Cell Biol. *13*, 438–443.

Bear, C.E., Li, C.H., Kartner, N., Bridges, R.J., Jensen, T.J., Ramjeesingh, M., and Riordan, J.R. (1992). Purification and functional reconstitution of the cystic fibrosis transmembrane conductance regulator (CFTR). Cell *68*, 809–818.

Cabral, C.M., Choudhury, P., Liu, Y., and Sifers, R.N. (2000). Processing by endoplasmic reticulum mannosidases partitions a secretion-impaired glycoprotein into distinct disposal pathways. J. Biol. Chem. *275*, 25015–25022.

Cabral, C.M., Liu, Y., Moremen, K.W., and Sifers, R.N. (2002). Organizational diversity among distinct glycoprotein endoplasmic reticulum-associated degradation programs. Mol. Biol. Cell *13*, 2639–2650.

Cabral, C.M., Liu, Y., and Sifers, R.N. (2001). Dissecting glycoprotein quality control in the secretory pathway. Trends Biochem. Sci. *26*, 619–624.

Chen, E.Y., Bartlett, M.C., and Clarke, D.M. (2000). Cystic fibrosis transmembrane conductance regulator has an altered structure when its maturation is inhibited. Biochemistry *39*, 3797–3803.

Chen, Y., Le, C.F., and Chuck, S.L. (1998). Calnexin and other factors that alter translocation affect the rapid binding of ubiquitin to apoB in the Sec61 complex. J. Biol. Chem. *273*, 11887–11894.

Cheng, S.H., Gregory, R.J., Marshall, J., Paul, S., Souza, D.W., White, G.A., O'Riordan, C.R., and Smith, A.E. (1990). Defective intracellular transport and processing of CFTR is the molecular basis of most cystic fibrosis. Cell *63*, 827–834.

Cozens, A.L., Yezzi, M.J., Kunzelmann, K., Ohrui, T., Chin, L., Eng, K., Finkbeiner, W.E., Widdicombe, J.H., and Gruenert, D.C. (1994). CFTR expression and chloride secretion in polarized immortal human bronchial epithelial cells. Am. J. Respir. Cell Mol. Biol. *10*, 38–47.

Danilczyk, U.G., and Williams, D.B. (2001). The lectin chaperone calnexin utilizes polypeptide-based interactions to associate with many of its substrates in vivo. J. Biol. Chem. *276*, 25532–25540.

Denning, G.M., Anderson, M.P., Amara, J.F., Marshall, J., Smith, A.E., and Welsh, M.J. (1992). Processing of mutant cystic fibrosis transmembrane conductance regulator is temperature-sensitive. Nature *358*, 761–764.

Drumm, M.L., Wilkinson, D.J., Smit, L.S., Worrell, R.T., Strong, T.V., Frizzell, R.A., Dawson, D.C., and Collins, F.S. (1991). Chloride conductance expressed by delta F508 and other mutant CFTRs in *Xenopus* oocytes. Science *254*, 1797–1799.

Elbashir, S.M., Harborth, J., Lendeckel, W., Yalcin, A., Weber, K., and Tuschl, T. (2001). Duplexes of 21-nucleotide RNAs mediate RNA interference in cultured mammalian cells. Nature *411*, 494–498.

Ellgaard, L., and Helenius, A. (2003). Quality control in the endoplasmic reticulum. Nat. Rev. Mol. Cell. Biol. *4*, 181–191.

Fuller, W., and Cuthbert, A.W. (2000). Post-translational disruption of the delta F508 cystic fibrosis transmembrane conductance regulator (CFTR)-molecular chaperone complex with geldanamycin stabilizes delta F508 CFTR in the rabbit reticulocyte lysate. J. Biol. Chem. *275*, 37462–37468.

Gelman, M.S., Kannegaard, E.S., and Kopito, R.R. (2002). A principal role for the proteasome in endoplasmic reticulum-associated degradation of misfolded intracellular cystic fibrosis transmembrane conductance regulator. J. Biol. Chem. *277*, 11709–11714.

Ghadially, F.N. (1996). Ultrastructural Pathology of the Cell and Matrix, 4th ed., British Library Cataloguing in Publication Data.

Hosokawa, N., Wada, I., Hasegawa, K., Yorihuzi, T., Tremblay, L.O., Herscovics, A., and Nagata, K. (2001). A novel ER alpha-mannosidase-like protein accelerates ER-associated degradation. EMBO Rep. *2*, 415–422.

Ihara, Y., Cohen-Doyle, M.F., Saito, Y., and Williams, D.B. (1999). Calnexin discriminates between protein conformational states and functions as a molecular chaperone in vitro. Mol. Cell *4*, 331–341.

Jakob, C.A., Burda, P., Roth, J., and Aebi, M. (1998). Degradation of misfolded endoplasmic reticulum glycoproteins in *Saccharomyces cerevisiae* is determined by a specific oligosaccharide structure. J. Cell Biol. *142*, 1223–1233.

Jensen, T.J., Loo, M.A., Pind, S., Williams, D.B., Goldberg, A.L., and Riordan, J.R. (1995). Multiple proteolytic systems, including the proteasome, contribute to CFTR processing. Cell *83*, 129–135.

Johnston, J.A., Ward, C.L., and Kopito, R.R. (1998). Aggresomes: a cellular response to misfolded proteins. J. Cell Biol. *143*, 1883–1898.

Kamhi, N.S., Shenkman, M., Tolchinsky, S., Fromm, S.V., Ehrlich, R., and Lederkremer, G.Z. (2001). A novel quality control compartment derived from the endoplasmic reticulum. Mol. Biol. Cell *12*, 1711–1723.

Kaufman, R.J. (1999). Stress signaling from the lumen of the endoplasmic reticulum: coordination of gene transcriptional and translational controls. Genes Dev. *13*, 1211–1233.

Kerem, B., Rommens, J.M., Buchanan, J.A., Markiewicz, D., Cox, T.K., Chakravarti, A., Buchwald, M., and Tsui, L.C. (1989). Identification of the cystic fibrosis gene: genetic analysis. Science *245*, 1073–1080.

Knittler, M.R., Dirks, S., and Haas, I.G. (1995). Molecular chaperones involved in protein degradation in the endoplasmic reticulum: quantitative interaction of the heat shock cognate protein BiP with partially folded immunoglobulin light chains that are degraded in the endoplasmic reticulum. Proc. Natl. Acad. Sci. USA *92*, 1764–1768.

Kopito, R.R., and Sitia, R. (2000). Aggresomes and Russell bodies. Symptoms of cellular indigestion? EMBO Rep. *1*, 225–231.

Lenk, U., Yu, H., Walter, J., Gelman, M.S., Hartmann, E., Kopito, R.R., and Sommer, T. (2002). A role for mammalian Ubc6 homologues in ER-associated protein degradation. J. Cell Sci. *115*, 3007–3014.

Li, C., Ramjeesingh, M., Reyes, E., Jensen, T., Chang, X., Rommens, J.M., and Bear, C.E. (1993). The cystic fibrosis mutation (delta F508) does not influence the chloride channel activity of CFTR. Nat. Genet. *3*, 311–316.

Loo, M.A., Jensen, T.J., Cui, L., Hou, Y., Chang, X.B., and Riordan, J.R. (1998). Perturbation of Hsp90 interaction with nascent CFTR prevents its maturation and accelerates its degradation by the proteasome. EMBO J. *17*, 6879–6887.

Lukacs, G.L., Mohamed, A., Kartner, N., Chang, X.B., Riordan, J.R., and Grinstein, S. (1994). Conformational maturation of CFTR but not its mutant counterpart (delta F508) occurs in the endoplasmic reticulum and requires ATP. EMBO J. *13*, 6076–6086.

Meacham, G.C., Lu, Z., King, S., Sorscher, E., Tousson, A., and Cyr, D.M. (1999). The Hdj-2/Hsc70 chaperone pair facilitates early steps in CFTR biogenesis. EMBO J. *18*, 1492–1505.

Meacham, G.C., Patterson, C., Zhang, W., Younger, J.M., and Cyr, D.M. (2001). The Hsc70 co-chaperone CHIP targets immature CFTR for proteasomal degradation. Nat. Cell Biol. *3*, 100–105.

Mezzacasa, A., and Helenius, A. (2002). The transitional ER defines a boundary for quality control in the secretion of tsO45 VSV glycoprotein. Traffic *3*, 833–849.

Molinari, M., Calanca, V., Galli, C., Lucca, P., and Paganetti, P. (2003). Role of EDEM in the release of misfolded glycoproteins from the calnexin cycle. Science *299*, 1397–1400.

Molinari, M., Galli, C., Piccaluga, V., Pieren, M., and Paganetti, P. (2002). Sequential assistance of molecular chaperones and transient formation of covalent complexes during protein degradation from the ER. J. Cell Biol. *158*, 247–257.

Oda, Y., Hosokawa, N., Wada, I., and Nagata, K. (2003). EDEM as an acceptor of terminally misfolded glycoproteins released from calnexin. Science *299*, 1394–1397.

Okiyoneda, T., *et al*. (2002). Calnexin Δ185–520 partially reverses the misprocessing of the ΔF508 cystic fibrosis transmembrane conductance regulator. FEBS Lett. *526*, 87–92.

Parodi, A.J. (2000). Protein glucosylation and its role in protein folding. Annu. Rev. Biochem. *69*, 69–93.

Pind, S., Riordan, J.R., and Williams, D.B. (1994). Participation of the endoplasmic reticulum chaperone calnexin (p88, IP90) in the biogenesis of the cystic fibrosis transmembrane conductance regulator. J. Biol. Chem. *269*, 12784–12788.

Riordan, J.R., *et al*. (1989). Identification of the cystic fibrosis gene: cloning and characterization of complementary DNA. Science *245*, 1066–1073.

Rommens, J.M., *et al*. (1989). Identification of the cystic fibrosis gene: chromosome walking and jumping. Science *245*, 1059–1065.

Saito, Y., Ihara, Y., Leach, M.R., Cohen-Doyle, M.F., and Williams, D.B. (1999). Calreticulin functions in vitro as a molecular chaperone for both glycosylated and non-glycosylated proteins. EMBO J. *18*, 6718–6729.

Schrag, J.D., Procopio, D.O., Cygler, M., Thomas, D.Y., and Bergeron, J.J. (2003). Lectin control of protein folding and sorting in the secretory pathway. Trends Biochem. Sci. *28*, 49–57.

Sferra, T.J., and Collins, F.S. (1993). The molecular biology of cystic fibrosis. Annu. Rev. Med. *44*, 133–144.

Tabcharani, J.A., Chang, X.B., Riordan, J.R., and Hanrahan, J.W. (1991). Phosphorylation-regulated Cl⁻ channel in CHO cells stably expressing the cystic fibrosis gene. Nature *352*, 628–631.

Takei, K., Mignery, G.A., Mugnaini, E., Sudhof, T.C., and De Camilli, P. (1994). Inositol 1,4,5-trisphosphate receptor causes formation of ER cisternal stacks in transfected fibroblasts and in cerebellar Purkinje cells. Neuron *12*, 327–342.

Tsui, L.C. (1992). The spectrum of cystic fibrosis mutations. Trends Genet. *8*, 392–398.

Wada, I., Rindress, D., Cameron, P.H., Ou, W.J., Doherty, J.J., 2nd, Louvard, D., Bell, A.W., Dignard, D., Thomas, D.Y., and Bergeron, J.J. (1991). SSR alpha and associated calnexin are major calcium binding proteins of the endoplasmic reticulum membrane. J. Biol. Chem. *266*, 19599–19610.

Ward, C.L., Omura, S., and Kopito, R.R. (1995). Degradation of CFTR by the ubiquitin-proteasome pathway. Cell *83*, 121–127.

Wigley, W.C., Fabunmi, R.P., Lee, M.G., Marino, C.R., Muallem, S., DeMartino, G.N., and Thomas, P.J. (1999). Dynamic association of proteasomal machinery with the centrosome. J. Cell Biol. *145*, 481–490.

Wilson, C.M., Farmery, M.R., and Bulleid, N.J. (2000). Pivotal role of calnexin and mannose trimming in regulating the endoplasmic reticulum-associated degradation of major histocompatibility complex class I heavy chain. J. Biol. Chem. *275*, 21224–21232.

Wimer-Mackin, S., and Granger, B.L. (1996). Transmembrane domain mutations influence the cellular distribution of lysosomal membrane glycoprotein A. Biochem. Biophys. Res. Commun. *229*, 472–478.

Xiong, X., Chong, E., and Skach, W.R. (1999). Evidence that endoplasmic reticulum (ER)-associated degradation of cystic fibrosis transmembrane conductance regulator is linked to retrograde translocation from the ER membrane. J. Biol. Chem. *274*, 2616–2624.

Yamamoto, A., Masaki, R., and Tashiro, Y. (1996). Formation of crystalloid endoplasmic reticulum in COS cells upon overexpression of microsomal aldehyde dehydrogenase by cDNA transfection. J. Cell Sci. *109*, 1727–1738.

Yang, Y., Janich, S., Cohn, J.A., and Wilson, J.M. (1993). The common variant of cystic fibrosis transmembrane conductance regulator is recognized by hsp70 and degraded in a pre-Golgi nonlysosomal compartment. Proc. Natl. Acad. Sci. USA *90*, 9480–9484.

Yoo, J.S., Moyer, B.D., Bannykh, S., Yoo, H.M., Riordan, J.R., and Balch, W.E. (2002). Non-conventional trafficking of the cystic fibrosis transmembrane conductance regulator through the early secretory pathway. J. Biol. Chem. *277*, 11401–11409.

Yoshida, Y., *et al*. (2002). E3 ubiquitin ligase that recognizes sugar chains. Nature *418*, 438–442.

Zapun, A., Petrescu, S.M., Rudd, P.M., Dwek, R.A., Thomas, D.Y., and Bergeron, J.J. (1997). Conformation-independent binding of monoglucosylated ribonuclease B to calnexin. Cell *88*, 29–38.

Zeitlin, P.L., Lu, L., Rhim, J., Cutting, G., Stetten, G., Kieffer, K.A., Craig, R., and Guggino, W.B. (1991). A cystic fibrosis bronchial epithelial cell line: immortalization by adeno-12-SV40 infection. Am. J. Respir. Cell Mol. Biol. *4*, 313–319.